ORIGINAL CONTRIBUTION

The effect of pre-shear on the extensional rheology of wormlike micelle solutions

**Avinash Bhardwaj · David Richter ·
Manojkumar Chellamuthu · Jonathan P. Rothstein**

Abstract The effect of initial microstructural deformation, alignment, and morphology on the response of wormlike micelle solutions in transient uniaxial extensional flows is investigated using a pre-shear device attached to a filament stretching rheometer. In filament stretching experiments, increasing the strength and the duration of the pre-shear just before stretch is found to delay the onset of strain hardening. In these experiments, the wormlike micelle solution filaments fail through a rupture near the axial midplane. The value of the elastic tensile stress at rupture is found to decrease with increasing pre-shear rate and duration. The most dramatic effects are observed at shear rates for which shear banding has been independently observed. The reduction in the strain hardening suggests that pre-shear before filament stretching might break down the wormlike micelles reducing their size before stretch. Strain hardening is also observed in capillary breakup rheometry experiments; however, the pre-sheared wormlike micelle solutions strain harden faster, achieve larger steady-state extensional viscosities and an increase in the extensional relaxation time with increasing shear rate and duration. The difference between the response of the wormlike micelles in filament stretching and capillary breakup experiments demonstrates the sensitivity of these self-assembling micelle networks to pre-conditioning.

A. Bhardwaj · D. Richter · M. Chellamuthu · J. P. Rothstein (✉)
Department of Mechanical and Industrial Engineering,
University of Massachusetts,
Amherst, MA 01003, USA
e-mail: rothstein@ecs.umass.edu

Introduction

Surfactants are currently used in a variety of applications including many household and cosmetic products, industrial viscosity modifiers in paints, detergents and pharmaceuticals, emulsifiers, encapsulants, and lubricants. In addition to these more common and recognizable products, visco-elastic surfactant technology has also become important in a wide range of applications including agrochemical spraying, inkjet printing, and enhanced oil recovery where they are used as polymer-free aqueous fracturing fluids in oilfield applications including drilling and reservoir stimulation (Kefi et al. 2004). Surfactants are molecules that consist of a hydrophilic head group and a hydrophobic tail. When dissolved in water above their critical micellar concentration (CMC), they can spontaneously self-assemble into large aggregates called micelles (Israelachvili 1985; Larson 1999; Rehage and Hoffmann 1991). As seen in Fig. 1, the resulting aggregate morphology can range from spherical micelles, to cylindrical micelles, and to more complex shapes like vesicles or lamellae depending on surfactant and counterion concentrations, ionic strength, and interaction (Lequeux and Candau 1997). Cylindrical micelles can grow into very long wormlike micelles with increasing surfactant concentration. Because of their long flexible structure, these worms can entangle and form a complex network, much like polymer melts. However, unlike polymer chains, which are covalently bonded along their backbones, a wormlike micelle is only held together by relatively weak physical attractions/repulsions, which can break and reform under Brownian motion. The dynamics of this ongoing and reversible breakup and reformation process is a strong function of surfactant and salt concentration, salinity, temperature, and flow (Cates 1990). This continuous breaking and reforming process
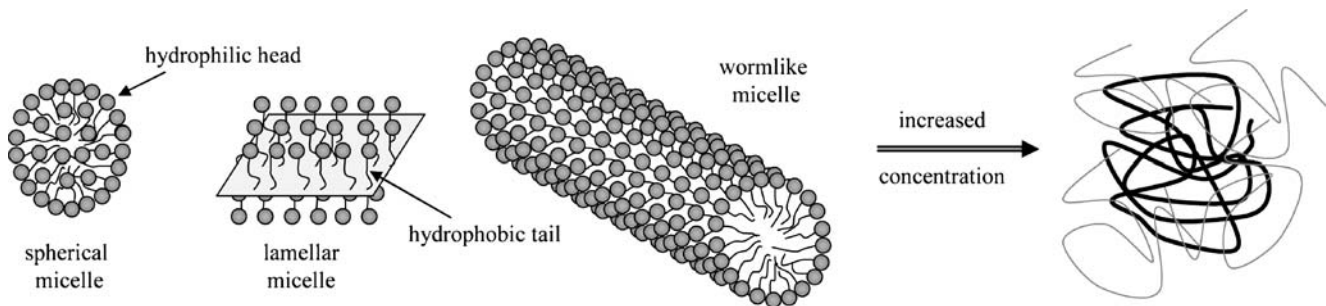
Fig. 1 Schematic diagram of wormlike micelle solutions showing various morphologies including spherical, lamellar, wormlike and long entangled wormlike micelles which can impart viscoelasticity

gives networks of wormlike micelles an additional relaxation mechanism besides reptation and results in a dynamic distribution of micelle lengths, which can change under an imposed shear or extensional flow making the resulting flow behavior even more complex then polymeric fluids (Cates and Turner 1990).

The linear viscoelastic behavior of these wormlike micelles can often be described by a single-mode Maxwell model (Rehage and Hoffmann 1991). In this fast-breaking limit, where the reptation time of the micelles are much longer than the breakup time of the micelles $\lambda_{\text{rep}} \gg \lambda_{\text{br}}$, Cates showed that the breakup and reptation time could be related to the measured value of the Maxwell relaxation time through $\lambda_M = (\lambda_{\text{rep}} \lambda_{\text{br}})^{1/2}$ (Cates 1987). However, the nonlinear viscoelastic response of these entangled micelle solutions in both shear and extension has been shown to be much more complex (Bhardwaj et al. 2007; Cates 1990; Khatory et al. 1993; Miller and Rothstein 2007; Rothstein 2003) and in need of further exploration.

The nonlinear behavior of surfactant wormlike micelles has been studied in shear flows of varying geometry for many years. In a steady shear flow at low shear rates, wormlike micelles demonstrate a Newtonian-like plateau in the shear viscosity. As the shear rate is increased, the viscosity begins to shear thin like a polymeric fluid. However, above a characteristic shear rate, the shear stress plateaus and can remain nearly constant over several decades of imposed shear rate (Berret 1997). Within this stress plateau, and with proper flow conditions, distinct shear bands of fluid at different local shear rates can develop. Fundamentally, it is clear that the high and low shear rate bands at a constant stress form in response to the need to preserve an average rate of strain across the flow profile (Mair and Calaghan 1996). Shear bands have been observed using several predominantly optical methods including flow-induced birefringence (FIB; Decruppe and Ponton 2003; Lee et al. 2005; Lerouge and Decruppe 2000), particle image velocimetry (PIV; Mendez-Sanchez et al. 2003; Miller and Rothstein 2007), light and neutron scattering (Berret et al. 1993; Kadoma and van Egmond 1998), and magnetic resonance imaging (Britton and

Callaghan 1999; Mair and Calaghan 1996). Several explanations for the observed shear banding have been proposed including stress-induced structure formation, stress-induced phase change from an isotropic to a nematic state, shear-induced demixing, or the consequence of an elastic flow instability (Grand et al. 1997; Hu et al. 1993; Huang et al. 1996; Wheeler et al. 1998). In complex flows, like the benchmark flow past a falling sphere (Chen and Rothstein 2004; Jayaraman and Belmonte 2003) and the flow through 4:1 contraction (Rothstein and McKinley 2001), although there are regions dominated by pure shear and pure extensional flow, understanding how preconditioning and microstructural changes of the entangled wormlike micelle network resulting from shear flows affect the response of these fluids in extensional flows can be critical to understanding the more complex flows experienced in commercial and industrial applications.

The first investigations of the extensional rheology of wormlike micelle solutions used an opposed jet device (Fischer et al. 1997; Lu et al. 1998; Prud'homme and Warr 1994; Walker et al. 1996). Prud'homme and Warr (1994) showed for a series of equimolar TTABr/NaSal solutions that at low extension rates, below the coil–stretch transition, a plateau in the steady-state extensional viscosity was observed corresponding to the Newtonian response. At higher extension rates, chain stretching within the oriented segments was observed to lead to strain hardening in the extensional rheology. At a critical Deborah number, the extensional viscosity was observed to reach a maximum and decreases with further increase in Deborah number. Prud'homme and Warr (1994) theorized that the observed reduction in the extensional viscosity at high extension rates was the result of a scission of the wormlike micelles in the strong extensional flow. This hypothesis was later supported by light scattering measurements (Chen and Warr 1997), which demonstrated a decrease in the radius of gyration of the micelle with the reduction in the extensional viscosity and the experiments of Rothstein (2003), which were able to quantify the energy required to scission wormlike micelles in strong extensional flows. Researchers have also used four-roll mills (Kato et al. 2002, 2004) and

the flow through porous media (Muller et al. 2004) to measure an apparent extensional viscosity of wormlike micelle solutions. Unfortunately, each of these devices has an unknown pre-strain history and some degree of shearing in the flow field. It is therefore very difficult to deconvolute the effect of shear on the measured stresses or clearly understand the importance of shear rate, extension rate, or accumulated strain on the resulting extensional viscosity calculation. There are thus two major issues that need to be addressed if we are to unambiguously understand how pre-shear history affects the extensional viscosity of wormlike micelle solutions. First is the need for an extensional rheometer that is capable of applying a shear-free homogeneous transient extensional flow on the fluid filament. This has been achieved with the recent development of the filament stretching extensional rheometer (FiSER; Anna et al. 2001; McKinley and Sridhar 2002; Sridhar et al. 1991; Tirtaatmadja and Sridhar 1993) and, to a lesser extent, the capillary breakup extensional rheometer (CaBER; Anna and McKinley 2001; Bazilevsky et al. 1990; Entov and Hinch 1997; Stelter et al. 2000) which produces a shear-free uniaxial extensional flow, which is unfortunately inhomogeneous in nature. The second issue that must be addressed is the need to precisely control the pre-deformation history of the wormlike micelles. This is accomplished using a servo motor to rotate the upper endplate of the filament stretching rheometer at a constant rate just before the onset of stretch making it possible to unambiguously characterize the effect of the initial microstructural deformation, alignment and morphology of the fluid filament on the extensional rheology or wormlike micelle solutions.

Rothstein (2003) used a filament stretching rheometer to measure the extensional rheology of a series of cetyltrimethylammonium bromide (CTAB) and sodium salicylate (NaSal) wormlike micelle solutions. Bhardwaj et al. (2007) later investigated the extensional rheology of a series of cetylpyridinium chloride (CPyCl) and NaSal as well as CTAB/NaSal wormlike micelle solutions using both a FiSER and a CaBER. These fluids were all found to demonstrate considerable strain hardening in the extensional viscosity with increasing accumulated strain (Bhardwaj et al. 2007; Rothstein 2003). Additionally, above a critical extension rate, the filament stretching experiments were all observed to come to an abrupt end with the dramatic rupture of the fluid filament near its axial midplane (Bhardwaj et al. 2007; Chen and Rothstein 2004; Rothstein 2003). This instability is unique to self-assembling viscoelastic systems; similar rupture events were also observed for associative polymer solutions in filament stretching experiments (Tripathi et al. 2006) and wormlike micelle solutions in pendent drop experiments (Smolka and Belmonte 2003). At the surfactant concentrations used in these experiments, the wormlike micelles have been shown

to be entangled forming a heavily interconnected, sometimes branched, networks (Appell et al. 1992; Handzy and Belmonte 2004; In et al. 1999). The failure of the fluid filament likely stems from the scission of wormlike micelles resulting in a dramatic breakdown of the micelle network structure en masse (Rothstein 2003). These flow instabilities have also been found to lead to new and interesting instabilities in more complex flows such as in the extensional flow in the wake of a sphere falling through a wormlike micelle solution (Chen and Rothstein 2004; Jayaraman and Belmonte 2003) or through an associative polymer solution (Mollinger et al. 1999), and the extensional flow in the wake of a bubble rising through a wormlike micelle solution (Handzy and Belmonte 2004) and has great significance to industrial flows of wormlike micelle solutions such as in turbulent drag reduction where strong extensional flow are often encountered. In all these complex flows, the fluid elements experience some degree of pre-shear before being stretched in strong extensional flows. Understanding the affect of pre-shear on this new class of flow instabilities unique to self-assembling systems is therefore important if we are to truly understand their impact on complex flows.

Although little is known about the effect of pre-shear on the extensional rheology of wormlike micelle solutions, there have been some experiments performed on polymer solutions. Brownian dynamics simulations of dilute polymer solutions and optical tweezers experiments on DNA and have shown that the transient evolution of macromolecular microstructure is very sensitive to the initial configuration of the macromolecule, a concept known as 'molecular individualism' (Doyle et al. 1998; Smith and Chu 1998). Brownian dynamics simulations have shown that the imposition of either an oscillating extensional field or a pre-shear in the direction of stretch on a polymer solution reduces the occurrences of kinks and folds resulting in faster stretching during subsequent extensional flows (Larson 2000). Larson (2000) showed, however, that the imposition of shear during stretch did not reduce the number of folded configurations. Several studies have attempted to experimentally quantify the effect of pre-shear history on the response of complex fluids in extensional flows (Anna 2000). For James et al. (1987) and Vissmann and Bewersdorff (1990), the resulting extensional and pre-shearing flows were inhomogeneous and a true extensional viscosity could not be determined. However, the work of Anna (2000), which used a pre-shear device attached to the upper plate of a filament stretching rheometer, was able to quantitatively determine the effect of pre-shearing on the extensional behavior of a series of polystyrene Boger fluids. Anna's experiments demonstrated that the pre-shear normal to the stretch direction results in a delay of the onset of strain hardening of the extensional viscosity, while a pre-

deformation parallel to the stretch direction hastens the onset of strain hardening—a result that is confirmed by FENE-P and the Brownian dynamic simulations of Larson (2000, 2005) and Agarwal (2000). No experiments or simulations have been performed to date to investigate the effect of pre-shear and the extensional rheology of wormlike micelle solutions in a controlled way. The results reported in this manuscript are the first such results.

In the experiments described within this manuscript, we investigate the effect of pre-shear history on the extensional rheology measurement of three different wormlike micelle solutions using both a FiSER and a CaBER. The outline of this paper is as follows. In Experimental setup, we briefly describe the implementation of the FiSER and the CaBER, the pre-shear device, the test fluids used, and their shear rheology. In Capillary breakup extensional rheometry (Results and discussion), we discuss the effect of pre-shear on the transient homogeneous uniaxial extensional rheology measured through filament stretching. In the same section, we discuss the effect of pre-shear on the extensional rheology of the test fluids measured through capillary breakup. Finally, we conclude in the last section.

Experimental setup

Test fluids

A series of wormlike micelle solutions assembled from two different surfactant/salt combinations were chosen for this study. The first set of wormlike micelle solutions that were tested were made up of the cationic surfactant CPyCl (Fisher Scientific) and NaSal (Fisher Scientific) dissolved in a brine of 100 mM NaCl in distilled water. For reasons described in (Miller and Rothstein 2007), the molar of surfactant to the binding salt was held fixed at (CPyCl)/(NaSal)=2. The addition of the salt helps screen the charges on the hydrophilic head groups of the surfactant making the resulting micelle more flexible (Kern et al. 1994). The electrostatic screening of the salt has been observed to lower the CMC for CPyCl in aqueous NaCl of CMC=0.9 mM to 0.12 mM (Lee et al. 2005). CPyCl and NaSal were obtained in dry form from Fisher Scientific. Molar concentrations of CPyCl between 50 and 100 mM were dissolved in brine on a hot plate with a magnetic stirring bar. During mixing, a moderately elevated temperature was applied to reduce viscosity and aid in uniform mixing. After the solutions were fully dissolved, approximately 20–30 min, they were allowed to settle at room temperature for at least 24 h before any experiments were performed to allow air bubbles introduced during mixing to rise out.

The second set of test fluids was a series of wormlike micelle solutions were made up of another cationic surfactant CTAB (Fisher Scientific) and NaSal in deionized water. As has been customary in the literature (Shikata and Kotaka 1991), the molar ratio of surfactant to the binding salt was held fixed at (CTAB)/(NaSal)=1, and the molar concentration of the CTAB was set at 50 mM. This solution is well above the critical micelle concentration, which for CTAB in pure water is CMC=0.9 mM and is again significantly lower in the presence of salt (Israelachvili 1985). The solution was prepared in the manner described above. At the concentration used, the wormlike micelle solution is concentrated and entangled with significant number of entanglement points per chain (Israelachvili 1985).

When analyzing and presenting the experimental data, the relaxation times and viscosities were adjusted to their values at a reference temperature of T_{ref}=25 °C using time–temperature superposition with a shift factor, a_T, defined by the Arrhenius equation (Bird et al. 1987). Within the temperature range of our experiments, the Arrhenius form of the time–temperature superposition shift factor was found to be in good agreement with the rheological data for each of the wormlike micelle solutions tested; however, because of the sensitivity of the underlying wormlike micelle structure to temperature, every effort was made to maintain the fluid temperature at precisely 25 °C plus or minus a few tenths of a degree for all of the extensional rheology measurements presented in this manuscript.

Shear rheometry

The steady and dynamic shear rheology of the test fluids was characterized using a stress-controlled rheometer (TA instruments, AR2000) with a 6 cm/2° cone-and-plate geometry. The micelle solutions were loaded and allowed to equilibrate for several minutes. The samples were not pre-sheared. In Fig. 2, the storage modulus, G', and loss modulus, G'', of the CPyCl/NaSal and the CTAB/NaSal wormlike micelle solutions are plotted as a function of angular frequency, ω, along with the prediction of a two-mode Maxwell model for CPyCl and a single-mode Maxwell model for CTAB. The viscoelastic properties of the fluids including zero shear rate viscosity, η_0, Maxwell relaxation time, λ, and the elastic plateau modulus, G_N^0, are listed in Table 1. The deviation of the rheological data from the predictions of the single mode Maxwell model observed at large angular frequencies in Fig. 2b correspond to the Rouse-like behavior of the micelle between entanglement points (Fischer and Rehage 1997) and can be used to determine both the breakup time, λ_{br}, and the reptation time, λ_{rep}, of the wormlike micelle chains. In the fast breaking limit $\lambda_{rep} \gg \lambda_{br}$, Cates showed that the breakup and reptation time could be related to the measured value of the Maxwell relaxation time through $\lambda=(\lambda_{rep}\lambda_{br})^{1/2}$ (Cates 1987).
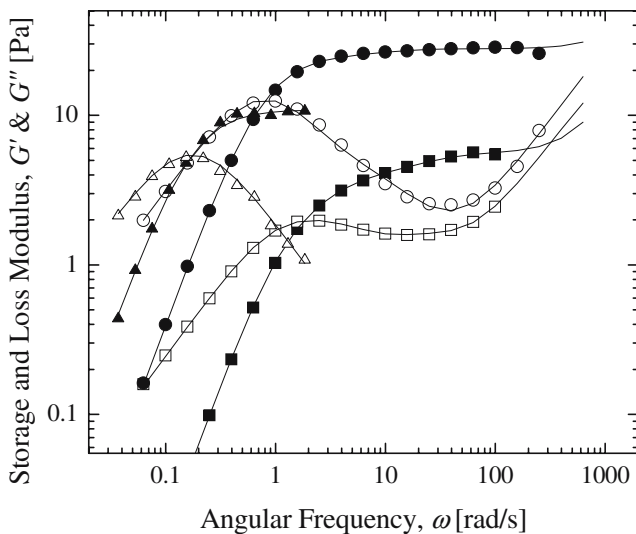
Fig. 2 Small amplitude oscillatory rheology of CPyCl/NaSal solutions in 100 mM NaCl at $T=20$ °C and CTAB/NaSal solution at $T=25$ °C. The data in includes: storage modulus, G' (*filled symbols*), and loss modulus, G'' (*open symbols*), for CPyCl/NaSal, *filled squares*; 50/25 mM, *filled circles*; 100/50 mM with two-mode Maxwell model fits to each of the data sets (*line*). Also included is CTAB/NaSal data for *filled triangles*; 50/50 mM, with a single-mode Maxwell fits to the data set (*line*)

Fig. 3 Steady shear viscosity of CPyCl/NaSal solutions in 100 mM NaCl at $T=20$ °C and CTAB/NaSal solution at $T=25$ °C. The data includes CPyCl/NaSal for *filled squares*; 50/25 mM, *filled circles*; 100/50 mM. Also included is CTAB/NaSal data for *filled triangles*; 50/50 mM

Additionally, the theoretical mesh size $\zeta_m=(kT/G_0)^{1/3}$ (Doi and Edwards 1986; Granek and Cates 1992) can be determined to gain some information about the proximity of entanglement points and the density of the wormlike micelle mesh.

In Fig. 3, the steady shear viscosity, η, is plotted as a function of shear rate, $\dot{\gamma}$. At small shear rates and angular frequencies, the micelle solutions have a constant zero shear rate viscosity. As the shear rate is increased, the fluid begins to shear thin. At a critical shear rate, the viscosity drops precipitously approaching a slope of $\eta \propto \dot{\gamma}^{-1}$. For the CPyCl/NaSal solutions, this plateau in the shear stress corresponds to the formation of two or more distinct shear bands. These shear bands have been recently measured and analyzed in our lab using PIV and FIB measurements and a specially designed large Couette flow cell (Miller and
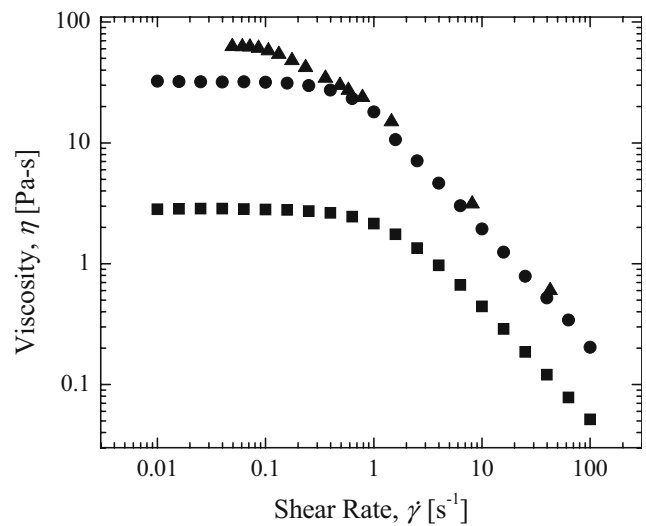
Rothstein 2007). The critical shear Weissenberg number for the onset of shear banding was found to be $Wi_{crit}=3.4$ and 2.0 for the 50/25 mM and 100/50 mM CPyCl/NaSal solutions, respectively. Although, we have not yet attempted to observe shear-banding in the CTAB/NaSal solutions, it could also account for the dramatic reduction in the shear viscosity observed in these systems and has been observed in the past for other CTAB solutions (Cappelaere et al. 1997; Drappier et al. 2006; Fischer and Callaghan 2001). For the data presented in Fig. 3, a critical shear Weissenberg number of about $Wi_{crit}=3.5$ is suggested for onset of shear banding in the 50/50 mM CTAB/NaSal solutions.

Filament stretching extensional rheometry

A filament FiSER capable of imposing a homogeneous uniaxial extension on a fluid filament placed between its two endplates was used to make simultaneously measurements of the evolution in the force and the midpoint radius. A complete description of the design and operating space of the filament stretching rheometer used in these experiments can be found in Rothstein and McKinley (Rothstein 2003; Rothstein and McKinley 2002a,b). Included in this filament stretching rheometer is a servo motor attached to the upper endplate capable of producing shear rates in the range of $0.1s^{-1} \leq \dot{\gamma} \leq 10s^{-1}$ at an initial gap of aspect ratio $\Lambda=H/R_0=1$. A schematic of the pre-shear device is shown in Fig. 4. The strength of the shear flow is defined by the shear Weissenberg number, $Wi_{shear} = \lambda\dot{\gamma}$, while the duration of the shear is defined by the shear Deborah number, $De_{shear}=\lambda/t_s$, where t_s is the duration of the imposed shear

Table 1 Parameters characterizing the rheology of the CPyCl/NaSal and CTAB/NaSal wormlike micelle solutions

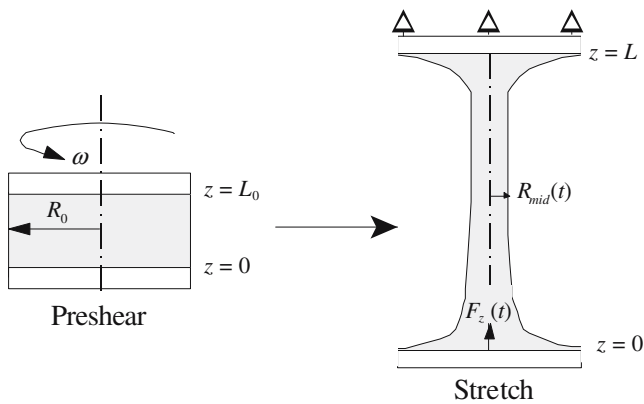|			CPyCl/NaSal (mM)		CTAB/NaSal (mM)
			50/25	100/50	50/50
Zero-shear viscosity	η_0	(Pa-s)	2.84	31.5	62
Plateau modulus	G_0	(Pa)	4.2	27	10.9
Relaxation time	λ	(s)	0.772	1.44	5.7

Fig. 4 Schematic diagram demonstrating the application of pre-shear before stretch in the filament stretching rheometer

flow (Bird et al. 1987). In this study, the use of the shear Deborah number is a little counterintuitive because increasing the duration of the pre-shear actually reduces the shear Deborah number. Additionally, the no pre-shear case results in an infinite Deborah number while an infinite pre-shear produces a Deborah number of zero. For that reason, we will often talk about the duration of pre-shear instead of the Deborah number and plot the inverse of the Deborah number, $\mathrm{De}_{\mathrm{shear}}^{-1} = t_s/\lambda$, so that the no pre-shear case corresponds to an inverse Deborah number of zero.

The goal of extensional rheometry is to cause a motion such that the resulting extension rate imposed on the fluid filament, $\dot{\varepsilon}$, is constant. The deformation imposed upon the fluid filament can be described in terms of a Hencky strain, $\varepsilon = -2 \ln (R_{\mathrm{mid}}/R_0)$, where R_0 is the initial midpoint radius of the fluid filament. The strength of the extensional flow is characterized by the extensional Weissenberg number, $\mathrm{Wi}_{\mathrm{ext}} = \lambda \dot{\varepsilon}$, which is the ratio of the characteristic relaxation time of the fluid, λ, to the characteristic time scale of the flow, $1/\dot{\varepsilon}_0$. The elastic tensile stress difference generated within the filament can be calculated from the algebraic sum of the total force measured by the load cell, F_z, if the weight of the fluid and the surface tension are taken into account while ignoring inertial effects (Szabo 1997)

$$\langle \tau_{zz} - \tau_{rr} \rangle = \frac{F_z}{\pi R_{mid}^2} + \frac{1}{2} \frac{\rho \mathrm{g} \left(\pi L_0 R_0^2 \right)}{\pi R_{mid}^2} - \frac{\sigma}{R_{mid}}, \qquad (1)$$

where L_0 is the initial endplate separation, σ is the equilibrium surface tension of the fluid, and ρ is the density of the fluid. The extensional viscosity may be extracted from the principle elastic tensile stress and is often non-dimensionalized as a Trouton ratio

$$Tr = \langle \tau_{zz} - \tau_{rr} \rangle \Big/ \eta_0 \dot{\varepsilon} = \eta_E^+/\eta_0, \qquad (2)$$

where η_E^+ is the transient extensional viscosity and η_0 is the zero shear rate viscosity of the fluid, respectively.

Capillary breakup extensional rheometry

To determine the extensional rheology of the less concentrated and less viscous fluids, capillary breakup extensional rheometry measurements (Anna and McKinley 2001; McKinley and Tripathi 2000; Rodd et al. 2005; Stelter et al. 2000) were performed using the filament stretching rheometer described above (Rothstein 2003; Rothstein and McKinley 2002b). In a CaBER, an initial nearly cylindrical fluid sample is placed between the two endplates of the filament stretching rheometer and stretched with an exponential profile, $L = L_0 \exp \left(\dot{\varepsilon}_0 t \right)$, to final length of L_{f}. The stretch is then stopped, and the capillary thinning of the liquid bridge formed between the two endplates produces a uniaxial extensional flow that can be used to measure an apparent extensional viscosity. The final stretch length is chosen such that $L_{\mathrm{f}} = 3.6 \, R_0$ and the stretch rate is chosen such that it is greater than the characteristic relaxation time of the fluid, $\dot{\varepsilon} \gg 1/\lambda$, and also greater than the time scale for capillary drainage of the liquid bridge, $\dot{\varepsilon} \gg \sigma/\eta_0 R_0$ (Anna and McKinley 2001). It has been shown that CaBER is capable of measuring the extensional viscosity of fluids with shear viscosities as low as 70 mPa·s and relaxation times as low as 10 ms (Rodd et al. 2005). In addition, CaBER can reach extremely large Hencky strains limited only by the resolution of diameter measurement transducer. In our experiments, a laser micrometer (Omron Z4LA) with a resolution of 5 μm was used to obtain final Hencky strains of up to $\varepsilon = 2 \ln \left(3\mathrm{mm}/5\mu m \right) = 12.7$, although in practice reliable measurements below 20 μm were difficult to achieve.

The breakup of the fluid filament is driven by capillary stresses and resisted by the extensional stresses developed within the flow. The extensional viscosity of the wormlike micelle solution can be determined by measuring the change in the filament diameter as a function of time. Papageorgiou (1995) showed that for a Newtonian fluid, the radius of the fluid filament will decay linearly with time, $R_{mid} (t) \propto (t_b - t)$. Conversely, Entov and Hinch (1997) showed that for an Oldroyd-B fluid, the radius will decay exponentially with time, $R_{mid} (t) \propto \exp(-t/3\lambda_E)$. The extension rate of the fluid filament is given by

$$\dot{\varepsilon} = -\frac{2}{R_{mid}(t)} \frac{dR_{mid}(t)}{dt} = \frac{2}{3\lambda_E}, \qquad (3)$$

and hence for an Oldroyd-B fluid, the flow has a constant extensional Weissenberg number of $\mathrm{Wi}_{\mathrm{ext}} = 2/3$. This value is larger than the critical extensional Weissenberg number of $\mathrm{Wi}_{\mathrm{ext}} = 1/2$ needed to achieve coil–stretch transition, and

thus, strain hardening of the extensional viscosity of the wormlike micelle solutions can be achieved. Additionally, the slope of the diameter as a function of time can be used to calculate a relaxation time in this elongational flow, λ_E. For Boger fluids, theory predictions and experiments show that $\lambda_E \approx \lambda$; however; for wormlike micelle solutions, strong deviations from this ideal value of the extensional relaxation time have recently been observed (Bhardwaj et al. 2007; Yesilata et al. 2006). An apparent extensional viscosity can be calculated by applying a force balance between capillary stresses and the elastic tensile stresses within the fluid filament (Anna and McKinley 2001)

$$\eta_E = \frac{\sigma/R_{mid}(t)}{\dot{\varepsilon}(t)} = \frac{-\sigma}{dD_{mid}/dt}. \tag{4}$$

To calculate the extensional viscosity, the diameter measurements are fit with the functional form proposed by Anna and McKinley (2001),

$$D_{mid}(t) = Ae^{-Bt} - Ct + E, \tag{5}$$

and differentiated with respect to time. The choices of fitting parameters have physical relevance. The decay of the fluid filament diameter at intermediate times can be related to the extensional relaxation time and the fitting parameter B such that $B = 1/3\lambda_E$. Additionally, C can be related to steady-state value of the extensional viscosity such that $C = \sigma/\eta_{E,\infty}$.

The equilibrium surface tension for each of the wormlike micelle solutions tested was assumed to be consistent with the value of $\sigma = 0.032$ and 0.036 N/m reported in the literature for the CPyCl/NaSal and CTAB/NaSal solutions above the CMC, respectively (Akers and Belmonte 2006; Cooper-White et al. 2002). However, in any free surface flow containing surfactants, one must also consider the role that dynamic surface tension could play. As the fluid filament is stretched and a new surface is generated, surfactant molecules diffuse from the bulk and populate the new surface. The result is a surface tension that is a function of the age of a given surface. Using a maximum bubble pressure tensiometer, Cooper-White et al. (2002) measured the dynamic surface tension of a series of CTAB/NaSal solutions. Above the CMC, the dynamic surface tension behavior was found to be independent of surfactant concentration. At short times, up to about 15 ms after the creation of a new surface, the dynamic surface tension equals that of water ($\sigma = 0.070$ N/m). As time progresses, the surface tension decays, eventually approaching an equilibrium value of $\sigma = 0.036$ N/m after about several hundred milliseconds (Cooper-White et al. 2002). Because the time scales of the CaBER experiments described here are slow compared to the time scale of the dynamic surface tension (seconds vs milliseconds), the equilibrium value of the surface tension

was used in all of our calculations of the extensional viscosity. Additionally, in the FiSER experiments, at the point that the fluid filament is stretching fast enough to necessitate the use of the dynamic surface tension in the force balance in Eq. 1, the elastic tensile stress typically dominates over the surface tension term and the factor of two change in the surface tension would make little to no difference in the final value of the extensional viscosity.

Results and discussion

Filament stretching extensional rheometry

Using the FiSER, a series of transient uniaxial extensional rheology experiments were performed on a number of wormlike micelle solutions with a well-defined pre-shear imposed just before stretch. The strength of the shear flow was modified by varying the shear rate or the Weissenberg number in shear, while the duration of the imposed shear was modified by varying the Deborah number in shear. To simplify this many variable problem, the strength of the extensional flow was fixed by keeping the extensional Weissenberg number constant for each of the wormlike micelle solutions tested. To insure that the wormlike micelles would undergo coil-stretch transition and strain harden, the extensional Weissenberg number was set to be much larger than $Wi_{ext} \gg 1/2$. The shear Weissenberg number was varied from a value less than one, $Wi_{shear} < 1$, where little micelle deformation and therefore little effect on the extensional rheology is expected to Weissenberg numbers larger than one, $Wi_{shear} > 1$, where shear thinning of the shear viscosity has begun to values larger than the critical Weissenberg number for the onset of shear banding, $Wi_{shear} > Wi_{crit}$, where dramatic changes to the micelle network have been observed and a significant effect on the extensional rheology is therefore expected. The impact of the duration of the imposed shear was likewise investigated by varying the inverse of the shear Deborah number from values much less than one, $De_{shear}^{-1} = t/\lambda \ll 1$, where the flow is not imposed long enough to produce much pre-conditioning of the wormlike micelles to values much larger than one, $De_{shear}^{-1} \gg 1$, where a steady-state shear flow has been established and any effects of pre-shear on the extensional viscosity should become apparent.

In Fig. 5a,b, the extensional viscosity is plotted as a function of Hencky strain for the 50/50 mM CTAB/NaSal wormlike micelle solution. Although a large number of shear rates were tested, two representative cases, $Wi_{shear} = 0.4$ and $Wi_{shear} = 4.6$, were chosen to be presented here to illustrate the effects of the lowest and highest shear rate regimes. For each of these two cases, the shear Deborah number was systematically varied between $0.40 \leq De_{shear} \leq 40$, the exten-
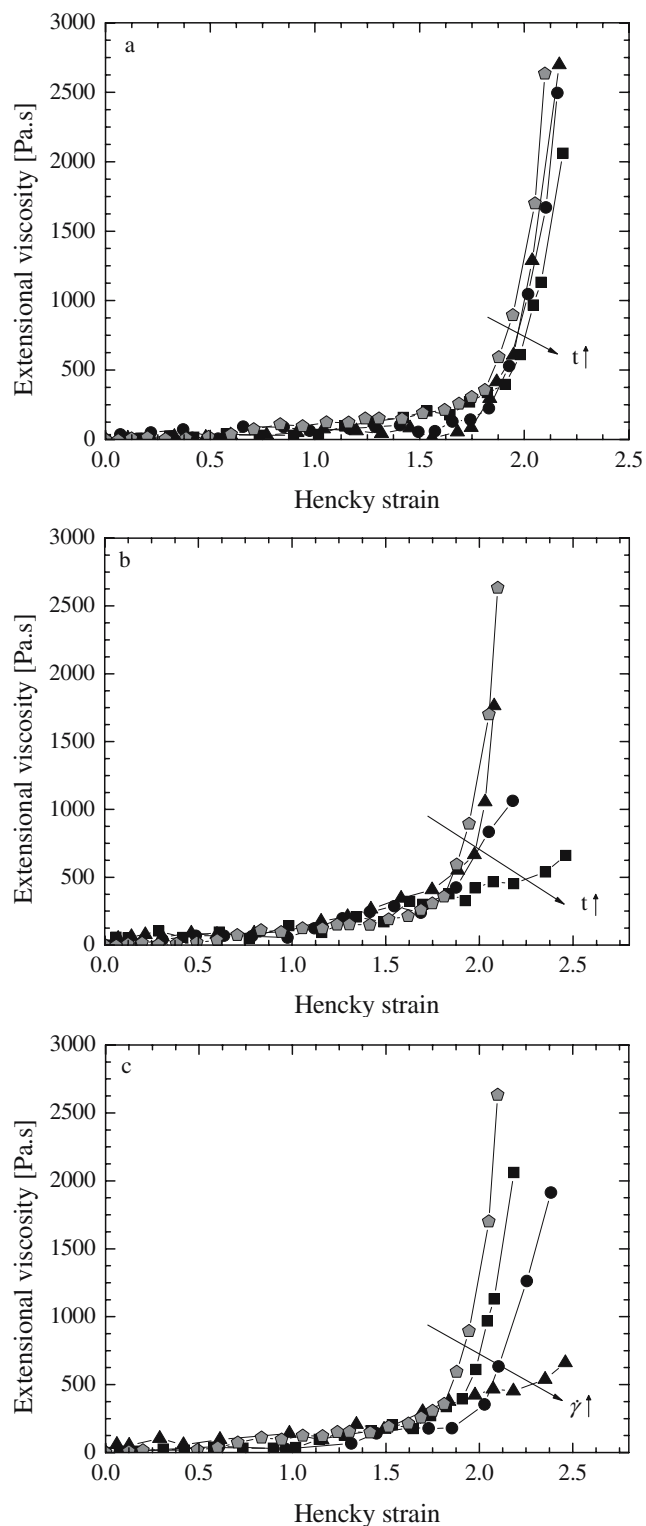
Fig. 5 The extensional viscosity as a function pre-shear strength and duration for the 50/50 mM CTAB/NaSal solution stretched at $Wi_{ext}=6.9$ with pre-shear values of **a** $Wi_{shear}=0.4$ and $0.40 \leq De_{shear} \leq 40$; **b** $Wi_{shear}=4.6$ and $0.40 \leq De_{shear} \leq 40$; and **c** $De_{shear}=0.40$ and $0.4 \leq Wi_{shear} \leq 4.6$. The *filled pentagon* corresponds to the case without pre-shear

sional Weissenberg number was held constant at $Wi_{ext}=6.9$, and the fluid temperature was maintained at $T=25$ °C for all of the experiments. In each figure, data from the no-pre-shear case is plotted with pentagons alongside the data from the pre-sheared experiments. For each of the filament stretching experiments described here, the fluid filaments all failed with a dramatic rupture near the axial midplane. This is consistent with the previous observations of Rothstein (Bhardwaj et al. 2007; Rothstein 2003). The dynamics of the filament rupture were captured and analyzed using a high-speed video camera (Phanton v.4.2). The dynamics of the final failure and the propagation of the fracture across the fluid filaments for the pre-sheared case were found to be similar to those observed by Rothstein in the absence of pre-shear (Bhardwaj et al. 2007; Rothstein 2003). However, as we will discuss in more detail below, the value of the extensional stress at failure was found to decrease with both increasing pre-shear strength and duration. As seen in Fig. 5, the extensional viscosity of the 50/50 mM CTAB/NaSal wormlike micelle solution was found to increase monotonically with increasing Hencky strain and demonstrated some degree of strain hardening for each of the filament stretching experiments. For the low shear rate case presented in Fig. 5a, $Wi_{shear}=0.4$, the pre-shear was found to have only a small effect on the subsequent extensional viscosity; producing a modest shift of the strain hardening of the extensional viscosity to larger Hencky strains and little change in the maximum value of the extensional viscosity achieved just before filament rupture. The magnitude of the shift was found to increase with increasing duration of the shear flow. Although this shift is rather small, it is outside of the experimental uncertainty, repeatable, and therefore significant. It is interesting to note that the magnitude of the shift in Fig. 5a is on the same order as the shift observed by Anna (2000) for dilute solutions of high molecular weight polystyrene, although their experiments were performed at shear Weissenberg numbers much larger than one, $Wi_{shear} \gg 1$. A physical interpretation that applies equally well to the results of pre-shear on the extensional flow response of polymer solutions and wormlike micelle solutions begins with the observation that the shear flow deforms and orients the micelles normal to the stretch direction. The delay in strain hardening can thus be explained as stemming from the need for the micelle to either rotate from the shear direction into the stretch direction or, alternately, to compress back through its equilibrium conformation before it is subsequently stretched. At the shear rates imposed in Fig. 5a, there does not seem to be any evidence that the shear flow is affecting the size, aggregation number or morphology of the micelles or the interconnectivity of the micelle network.

As can be seen in Fig. 5b, increasing the shear Weissenberg number to $Wi_{shear}=4.6$ has a dramatic effect on the extensional viscosity of the 50/50 mM CTAB/NaSal worm-

like micelle solution. As the duration of the pre-shear is increased, the strain hardening is delayed to larger Hencky strains. At a shear Deborah number of $De_{shear}=0.40$, the duration of the shear flow is $t_s=2.5\lambda$, and the strain hardening is delayed by nearly an entire Hencky strain unit. Additionally, although all the fluid filaments were found to rupture, the final extensional stress and viscosity is greatly reduced with increasing shear time. At this shear Weissenberg number, the steady shear rheology in Fig. 3 shows significant shear thinning and is suggestive of the presence of shear bands. Although we have demonstrated the existence of shear bands in the 50/25 mM and the 100/50 mM CPyCl/NaSal solutions (Miller and Rothstein 2007), we have not yet determined if the plateau in the shear stress with shear rate and the resulting precipitous shear thinning in the shear viscosity observed for the case of the 50/50 mM CTAB/NaSal wormlike micelle solution is the result of shear banding. The presence of shear bands would result in a spatial variation of micelle concentration, aggregation number, or morphology across the fluid filament at the onset of stretch. Additionally, the formation of shear bands is not instantaneous but can take on the order of a relaxation time to develop (Miller and Rothstein 2007). At the high pre-shear rates imposed upon the fluid filaments in Fig. 5b, the presence of a high shear rate band containing lower viscosity fluid comprised of shorter, less-extensible micelles broken down by the shear flow could account for the delay of the onset of strain hardening and the dramatic reduction in the extensional viscosity after prolonged pre-shearing of the fluid. If the presence of the shear banding is the root cause of the dramatic changes to the extensional viscosity with and without pre-shear, then at shear Weissenberg numbers where the fluid has begun to shear thin, but shear banding does not occur, one would not expect to observe as significant an impact of pre-shear on the extensional rheology. This is in fact confirmed in Fig. 5c.

In Fig. 5c, the response of the 50/50 mM CTAB/NaSal solution is plotted at a fixed shear Deborah number of $De_{shear}=0.40$ and varying the shear Weissenberg number between $0.4 \leq Wi_{shear} \leq 4.6$ at the same fixed value of the extensional Weissenberg number of $Wi_{ext}=6.9$. As expected, the shift of the strain hardening to larger Hencky strains and the reduction in the maximum extensional viscosity obtained before rupture were found to increase with increasing shear rate. The effect in the shear thinning region before the onset of shear banding, $Wi_{shear}=1.7$, is significant; however, it is the high Weissenberg number of $Wi_{shear}=4.6$ that shows the marked deviation from the no pre-shear data, demonstrating almost no strain hardening at all.

A quantitative comparison between the trends of the maximum extensional viscosity or equivalently the maximum elastic tensile stress achieved at the time of the fluid filament rupture is presented in Fig. 6 for a wide range of shear

Deborah number De_{shear} and the shear Weissenberg number Wi_{shear}. To make Fig. 6a easier to read, we plot extensional viscosity against one over the shear Deborah number so that $De_{shear}^{-1}=0$ is the no-pre-shear case, and increasing values along the x-axis correspond to increasing duration of pre-shear. The maximum extensional viscosity of the 50/50 mM CTAB/NaSal solutions at rupture is found to decrease quite quickly with increasing duration of pre-shear, eventually approaching an asymptotic value of about $\eta_E \approx 2000$ Pa·s at a shear Weissenberg number of $Wi_{shear}=0.40$ and a value $\eta_E \approx 500$ Pa·s at $Wi_{shear}=4.6$. At the largest shear Weissenberg numbers tested, the extensional viscosity at rupture appears to be very sensitive even to just a very short application of pre-shear, much shorter than the relaxation time of the fluid. At lower Weissenberg numbers, the fluid is significantly less sensitive and, as seen in Fig. 6a, approaches a larger asymptotic value closer to the no pre-shear value. At
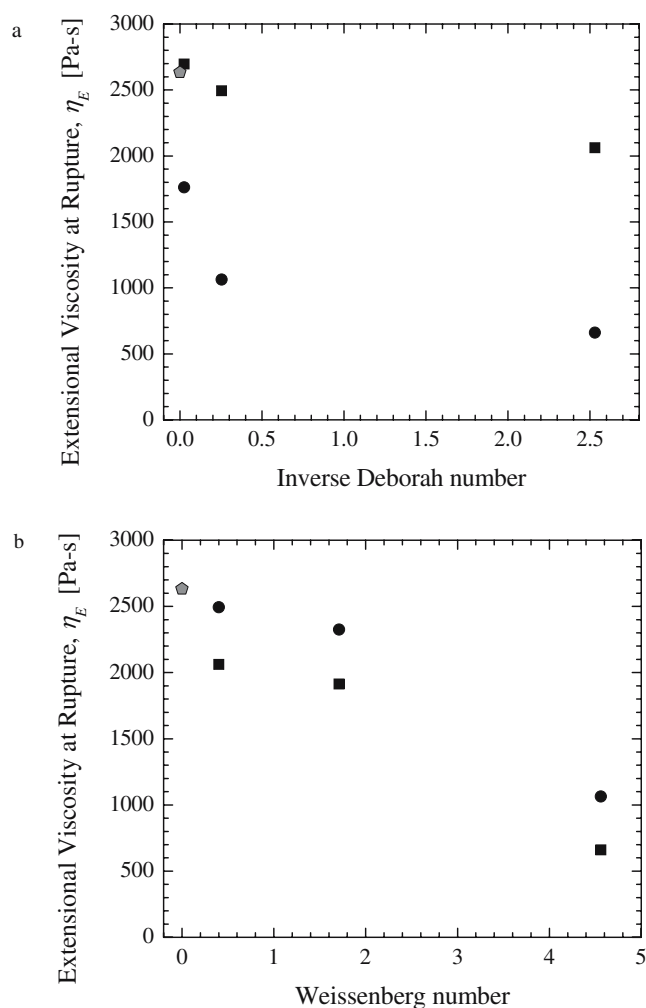

Fig. 6 The maximum extensional viscosity measured at filament rupture for 50/50 mM CTAB/NaSal stretched at $Wi_{ext}=6.9$ with pre-shear values of **a** $Wi_{shear}=0.40$ (*filled squares*) and 4.6 (*filled circles*); and **b** $De_{shear}=0.40$ (*filled circles*) and 4.0 (*filled squares*). The *filled pentagon* corresponds to the case without pre-shear

a fixed shear Deborah number as shown in Fig. 6b, the extensional viscosity at rupture appears to decay approximately linearly with increasing shear rate, whereas the duration of the pre-shear dictates how quickly the extensional viscosity decays. To put these observations into some perspective, it is important to note two things. First, that Anna and McKinley (Anna 2000); observed no discernable difference in the steady-state value of the extensional viscosity of polymer solutions with and without pre-shear. Second, and perhaps more significant, Bhardwaj et al. (2007) and Rothstein (2003) demonstrated that in the absence of pre-shear, both the CTAB/NaSal and CPyCl/NaSal wormlike micelle solutions ruptured at a constant value of elastic tensile stress, independent of extension rate. Thus, the tensile stress at failure appears to be an excellent indicator of the underlying wormlike micelle structure that is independent of the strength of the extensional flow but appears to be strongly dependent on the strength and duration of the shear flow applied just before the onset of the stretch. These results clearly demonstrate that even in the absence of shear banding, micelle or micelle network changes resulting from pre-shear can have a very strong effect on the response of wormlike micelle solutions in extensional flows.

To investigate the universality of the CTAB/NaSal observations, we extended our study to investigate the effect of pre-shear on the response of a series of CPyCl/NaSal wormlike micelle solutions in extensional flows. In Fig. 7a, the extensional viscosity of the 100/50 mM CPyCl/NaSal wormlike micelle solution is plotted against Hencky strain for a series of measurements taken at a fixed shear Weissenberg number of $Wi_{shear}=1.8$ and range of shear Deborah numbers varying between $0.1 \leq De_{shear} \leq 10$. The strength of the extensional flow was once again held fixed by maintaining a constant extensional Weissenberg number of $Wi_{ext}=5$ for all of the experiments in Fig. 7. As was observed previously for the CTAB/NaSal solutions, increasing the duration of the pre-shear was found to delay the onset of strain hardening and reduce the final extensional viscosity at rupture. As seen in Fig. 7b, by holding the shear Deborah number fixed at $De_{shear}=1.0$ and varying shear Weissenberg number between $0.1 \leq Wi_{shear} \leq 1.8$, the effect of shear rate was probed. The results of the CPyCl/NaSal solutions are consistent with the CTAB/NaSal solutions although perhaps slightly less pronounced for the values of pre-shear presented in Fig. 7. Increasing the shear rate was found to delay the onset of strain hardening and reduce the extensional tensile stress at rupture.

Capillary breakup extensional rheometry

In the capillary breakup extensional rheometry experiments described in this section, the filament stretching
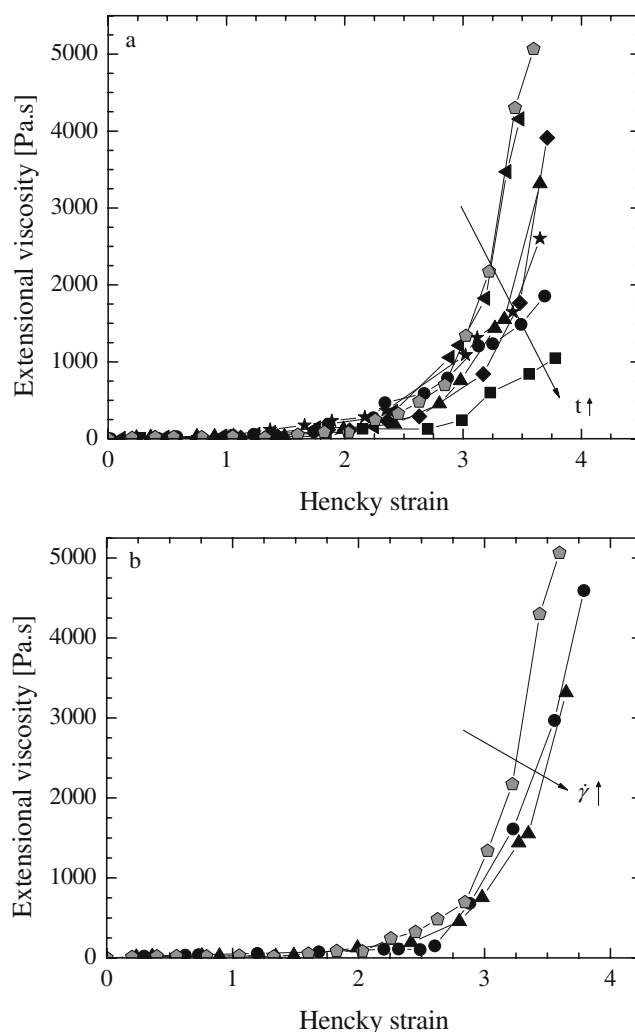

Fig. 7 The extensional viscosity as a function pre-shear strength and duration for the 100/50 mM CPyCl/NaSal solution stretched at $Wi_{ext}=5.0$ with pre-shear values of **a** $Wi_{shear}=1.8$ and $0.1 \leq De_{shear} \leq 10$; and **b** $De_{shear}=1.0$ and $0.1 \leq Wi_{shear} \leq 1.8$. The *filled pentagon* corresponds to the case without pre-shear

rheometer was used to impose a step extensional strain on an initially cylindrical sample after pre-conditioning it with a known strength and duration of pre-shear. The diameter was then monitored as the fluid filament thinned under capillary action. The measurements of the diameter as a function of time were used to determine both an extensional relaxation time and an apparent transient extensional viscosity for viscoelastic fluids with shear viscosities too thin or shear relaxation time too small to be measured using a filament stretching rheometry.

Representative plots of the diameter as a function of time are presented for the 50/50 mM CTAB/NaSal solution in Fig. 8 for a range of shear Weissenberg and shear Deborah numbers. The diameter data can be used to calculate an

apparent transient extensional viscosity using Eq. 5. The best fit of Eq. 5 to the diameter measurements is overlaid on the data in Fig. 8. We denote this extensional viscosity as apparent because unlike filament stretching experiments, the extension rate is not constant throughout the capillary break-up experiments but rather changes as the influence of finite extensibility becomes more pronounced at larger strains. In Fig. 8, the effect of pre-shear on the capillary-driven decay of the diameter with respect to time is illustrated by fixing the shear Weissenberg number at a relatively low value of $Wi_{shear}=0.57$ while varying the shear Deborah number between $0.40 \leq De_{shear} \leq 40$. As the duration of pre-shear is increased, the onset of strain hardening indicated by the linear decay of data on a semi-log plot is delayed to later times and larger strains. The no-pre-shear case is represented by pentagons and superimposed over this and each of the subsequent figures in this section.

The apparent extensional viscosity was calculated from the diameter measurements using Eq. 4. For the 50/50 mM CTAB/NaSal wormlike micelle solution, the extensional viscosity is presented in Fig. 9 for a wide range of shear Weissenberg and Deborah numbers. The data clearly demonstrate that pre-shear has a significant effect on the extensional viscosity measured in CaBER. In Fig. 9a, the shear Weissenberg number is maintained constant at $Wi_{shear}=0.4$ while the shear Deborah number was varied between $0.40 \leq De_{shear} \leq 40$. The steady-state value of the apparent extensional viscosity of the fluid filament was found to increase monotonically, and strain hardens earlier with decreasing duration of pre-shear. These results are in stark contrast with the results of filament stretching, which
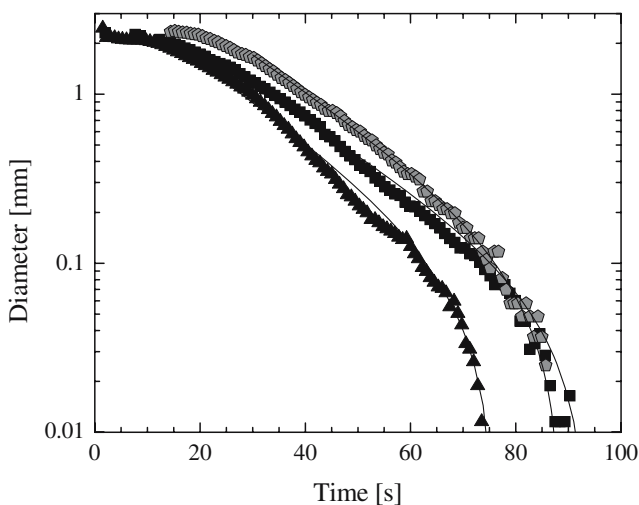

Fig. 8 The evolution in filament diameter for a series of CaBER experiments on the 50/50 mM CTAB/NaSal solution with pre-shear values of $Wi_{shear}=0.57$ and $0.40 \leq De_{shear} \leq 40$. The *filled pentagon* corresponds to the case with no pre-shear
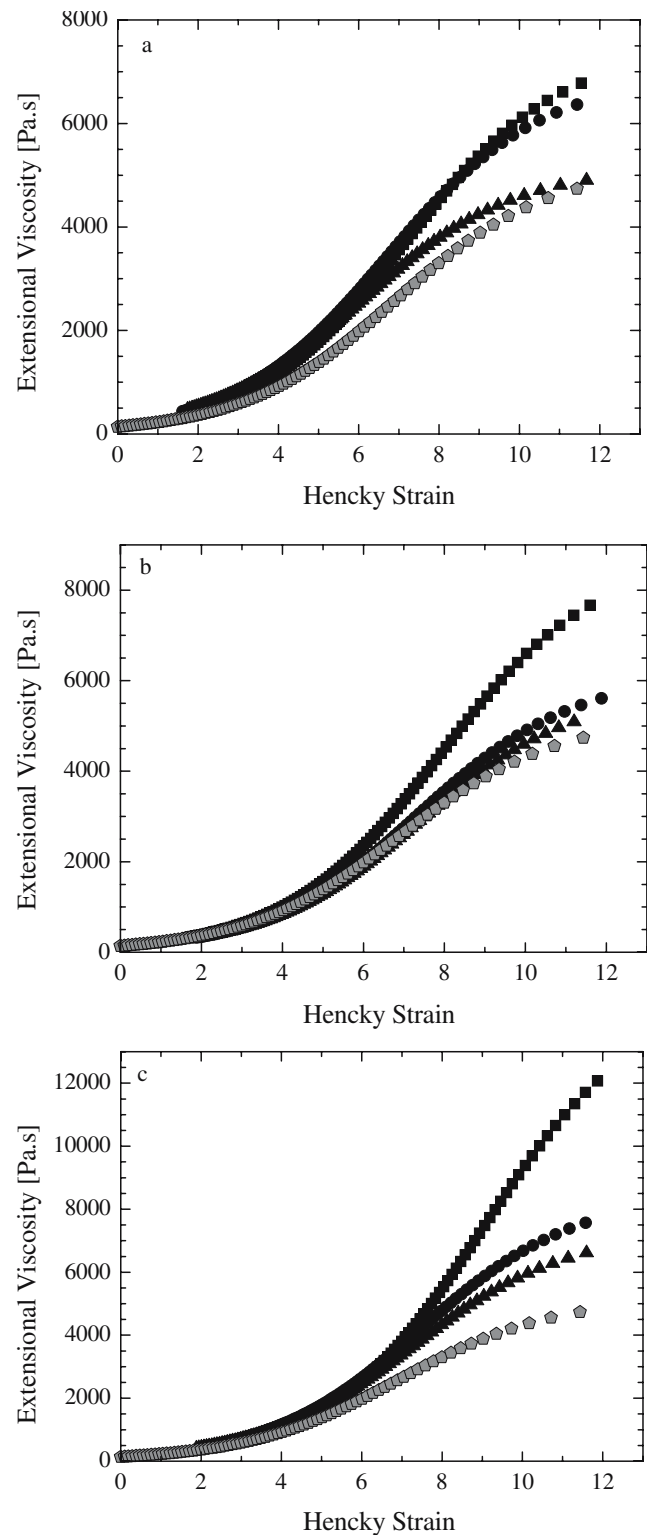

Fig. 9 Apparent extensional viscosity measurements for a series of CaBER experiments using the 50/50 mM CTAB/NaSal solution with shear Weissenberg numbers of **a** $Wi_{shear}=0.4$; **b** $Wi_{shear}=0.57$; and **c** $Wi_{shear}=1.71$. In each figure, the shear Deborah number is increased from (*filled square*) $De_{shear}=0.4$ to (*filled circles*) $De_{shear}=4$, and finally to (*filled triangles*) $De_{shear}=40$. The *filled pentagon* corresponds to the case without pre-shear

showed the opposite trends with both shear Deborah and shear Weissenberg number. These observations are reinforced by Fig. 9b and c, which contain data at shear Weissenberg numbers of $Wi_{shear}=0.57$ and $Wi_{shear}=1.71$, respectively. At $Wi_{shear}=0.4$ and $De_{shear}=40$, pre-shear is found to have little effect on the extensional rheology as it agrees quite well with the no-pre-shear case. This is not surprising considering that the total strain imposed on the fluid in this experiment, $\varepsilon = Wi_{shear}/De_{shear} = 0.01$, is well within the linear viscoelastic limit for this fluid, and little to no effect on the extensional viscosity is expected. Further increasing the duration of the shear or, as demonstrated in Fig. 10, further increasing the shear Weissenberg number results in increases to the apparent extensional viscosity until it finally approaches an asymptotic value. This behavior is non-intuitive and difficult to explain physically. What is clear is that CaBER measurements of wormlike micelle solutions are extremely sensitive to any amount of pre-conditioning. Even in the absence of pre-shear, the step strain imposed on the fluid filament in CaBER is essentially a pre-conditioning step parallel to the flow direction as the fluid is initially stretched at a very large extensional Weissenberg number, $Wi_{ext} \gg 1$, before the stretch is stopped and the fluid filament is allowed to drain under a capillary action at a nominal extensional Weissenberg number of $Wi_{ext} = 2/3$. The conventional wisdom in regards to CaBER measurements on polymer solutions is that the initial deformation induced by the step strain relaxes out quickly and does not affect the extensional rheology measurements (Anna and McKinley 2001). However, in self-assembled systems like wormlike micelle solutions, the initial step strain can affect the size or
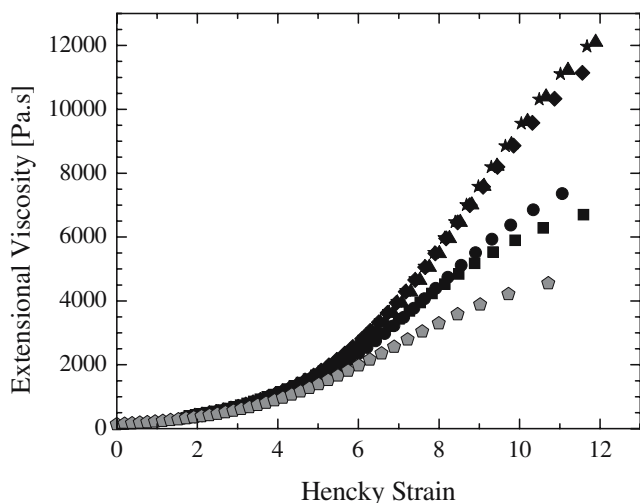
morphology of the micelle or the interconnectivity of the micelle network probed by CaBER. This initial pre-conditioning step might account for the dramatic under-prediction of the steady-state value of the extensional viscosity in the CaBER experiments when compared to the maximum extensional viscosities measured in FiSER at similar extension rates in the absence of pre-shear (Bhardwaj et al. 2007). Additionally, the interpretation of the results of pre-shear in CaBER becomes more difficult than in FiSER because the fluid filament experiences a pre-conditioning step normal to the flow direction followed by a pre-conditioning step parallel to the flow direction. One possible explanation is that the pre-shear alters the size or morphology of the micelle or the interconnectivity of the micelle network in such a way that it minimizes the effect of the step–stretch thereby allowing the extensional rheology measurements made in CaBER to approach the no pre-shear measurements in FiSER. The data in Figs. 9 and 10 and the CPyCl/NaSal figures that follow clearly demonstrate a complex interplay between these two pre-conditioning steps that we do not yet fully understand.

In Fig. 11, the effect of pre-shear on the apparent extensional viscosities for the 50/25 mM CPyCl/NaSal wormlike micelle solutions measured with the CaBER is presented. The trends for the CPyCl/NaSal solutions are consistent with the CTAB/NaSal solutions, an increase in the apparent extensional viscosity with increasing pre-shear strength and duration. Again, these observations are in stark contrast with the extensional rheology measured with the FiSER.

In addition to the apparent extensional viscosity, the effects of pre-shear on the extensional relaxation time can be probed using the value of $B = 1/3\lambda_E$ obtained from the best fit of Eq. 5 to the diameter decay data. The extensional relaxation time is plotted as a function of the inverse of the Deborah number for the 50/50 mM CTAB/NaSal solution in Fig. 12a and the 50/25 mM CPyCl/NaSal solution in Fig. 12b. The extensional relaxation time is found to decrease with increasing pre-shear duration; however, like the extensional viscosity, the relaxation time is found to increase with increasing shear rate. As one might expect, at shear times much larger than the relaxation time of the fluid, the value of the extensional relaxation time approaches an asymptotic limit. The no pre-shear limit is found to fit very well within the trends of the lowest shear Weissenberg number experiments. These observations are consistent for both fluids. In all cases, the extensional relaxation time is found to be significantly smaller than the longest relaxation time obtained from the linear viscoelasticity measurements, $\lambda_E \ll \lambda$. It is clear from these complex trends and observations that proper interpretation of CaBER data for wormlike micelle solutions with or even without
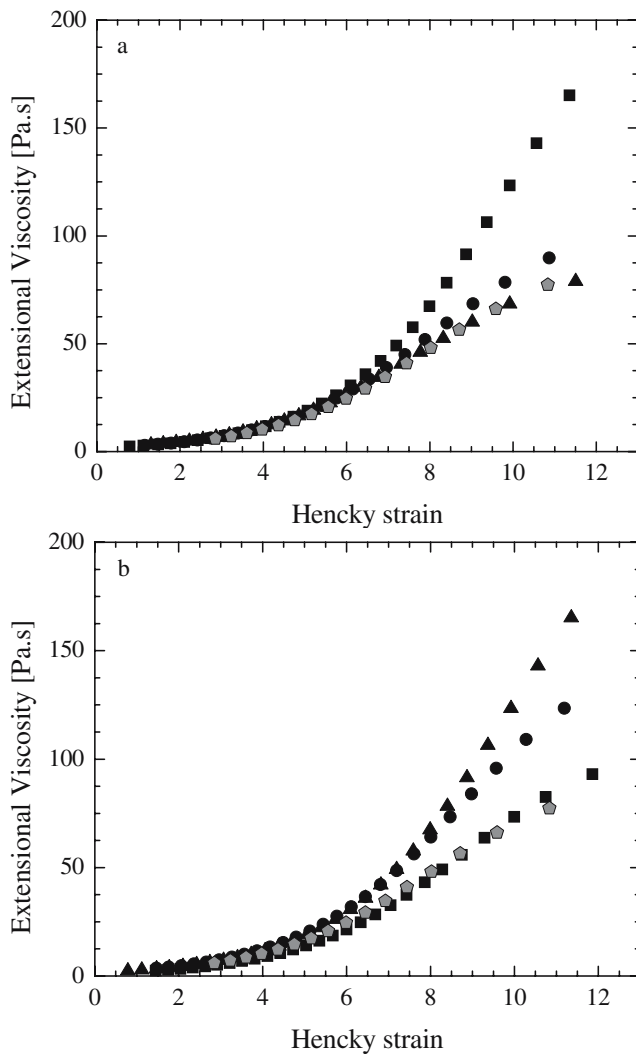

Fig. 10 Apparent extensional viscosity measurements for a series of CaBER experiments using the 50/50 mM CTAB/NaSal solution with $De_{shear}=0.4$ and (*filled squares*) $Wi_{shear}=0.4$, (*filled circles*) $Wi_{shear}=0.57$, (*filled triangles*) $Wi_{shear}=1.71$, (*filled diamonds*) $Wi_{shear}=4.55$, and (*filled stars*) $Wi_{shear}=7.0$. The *filled pentagon* corresponds to the case without pre-shear

Fig. 11 Apparent extensional viscosity measurements for a series of CaBER experiments on the 50/25 mM CPyCl/NaSal solution with pre-shear values of **a** $Wi_{shear}=0.95$ and (*filled squares*) $De_{shear}=0.053$, (*filled circles*) $De_{shear}=0.53$, and (*filled triangles*) $De_{shear}=5.3$; and **b** $De_{shear}=0.053$ and (*filled squares*) $Wi_{shear}=0.054$, (*filled circles*) $Wi_{shear}=0.62$, and (*filled triangles*) $Wi_{shear}=0.95$. The *filled pentagon* corresponds to the case with no pre-shear

Fig. 12 The extensional relaxation time extracted from CaBER measurements of **a** the 50/50 mM CTAB/NaSal solution with pre-shear values of (*filled circles*) $Wi_{shear}=0.57$, (*filled triangles*) $Wi_{shear}=1.71$, (*filled diamonds*) $Wi_{shear}=4.55$, (*filled stars*) $Wi_{shear}=7.0$; and **b** the 50/25 mM CPyCl/NaSal solution with pre-shear values of (*filled squares*) $Wi_{shear}=0.054$, (*filled circles*) $Wi_{shear}=0.23$, (*filled triangles*) $Wi_{shear}=0.62$, and (*filled diamonds*) $Wi_{shear}=0.95$. The *filled pentagon* corresponds to the case with no pre-shear

pre-shear is an extremely challenging problem. A more complete understanding of the response of these complex fluids may require the development of new constitutive models for wormlike micelle solutions.

Conclusions

The role of pre-shear on the extensional rheology of a series of wormlike micelle solutions was studied using both a filament stretching rheometer and capillary breakup rheometer. A number of different wormlike micelle solutions were tested including a 50/50 mM CTAB/NaSal solution in deionized water and a 100/50 mM and 50/25 mM CPyCl/
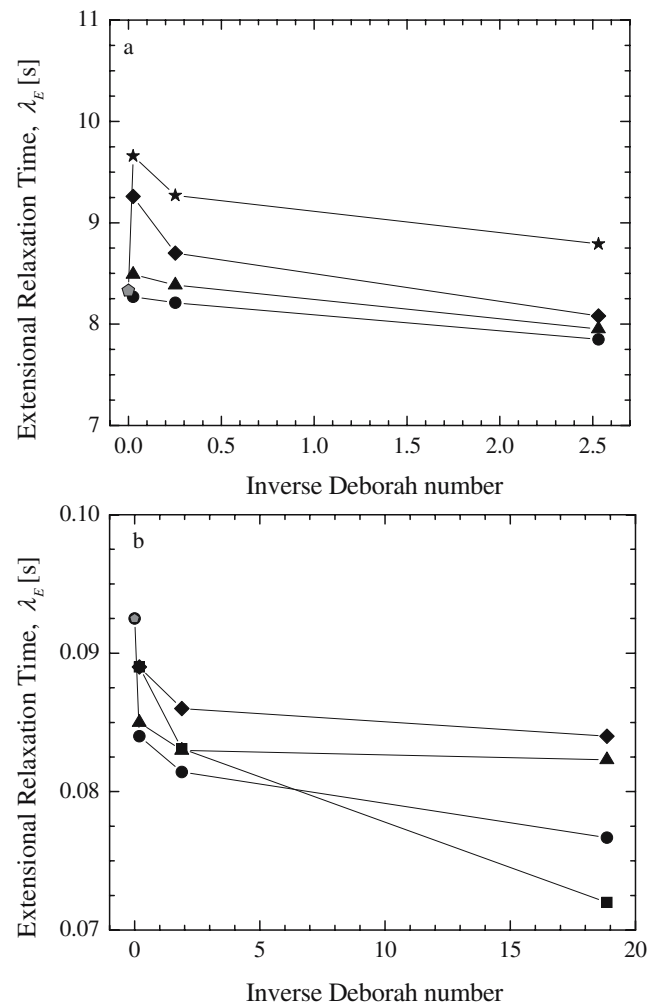
NaSal solution in a 100 mM aqueous NaCl solution. The shear rheology of each of the wormlike micelle solutions tested demonstrated Maxwell behavior in small amplitude oscillatory shear flow and shear banding at large shear rates in steady-shear experiments.

In transient homogeneous uniaxial extension imposed by a filament stretching rheometer, each of the wormlike micelle solutions demonstrated significant strain hardening. At large extension rates, the wormlike micelle solution filaments were all found to fail through a dramatic rupture near the axial midplane. Although the value of the elastic tensile stress at rupture was found to be independent of imposed extension rate for the no pre-shear case, the

maximum elastic tensile stress was found to reduce dramatically with increasing pre-shear rate and duration. In addition, increasing the strength and the duration of the pre-shear was found to result in a delay in the onset of strain hardening to larger Hencky strains. The most dramatic effects were observed at shear rates for which shear banding had been observed. The reduction in the strain hardening suggests that the pre-shear might reduce the size of the wormlike micelles or perhaps changes the interconnectivity of the micelle network before stretch.

The effect of pre-shear on the extensional viscosity measured in the capillary breakup rheometry experiments is very different from that observed in filament stretching. The wormlike micelle solutions were found to strain harden faster, achieve larger steady-state extensional viscosities and an increase in the extensional relaxation time with increasing pre-shear rate and duration. The difference between the response of the wormlike micelles in filament stretching and capillary breakup experiments demonstrates the sensitivity of these self-assembling micelle networks to pre-conditioning and highlights the difficulty in properly interpreting of CaBER data for wormlike micelle solutions with or without pre-shear. The development of a more complete understanding of the response of these complex fluids may require the development of new constitutive models for wormlike micelle solutions.

References

Agarwal US (2000) Effect of initial conformation, flow strength and hydrodynamic interaction on polymer molecules in extensional flows. J Chem Phys 113:3397–3403

Akers B, Belmonte A (2006) Impact dynamics of a solid sphere falling into a viscoelastic micellar fluids. J Non-Newton Fluid Mech 135:97–108

Anna SL (2000) "Filament stretching of model elastic liquids," Ph.D. Thesis, Harvard University

Anna SL, McKinley GH (2001) Elasto-capillary thinning and breakup of model elastic liquids. J Rheol 45:115–138

Anna SL, McKinley GH, Nguyen DA, Sridhar T, Muller SJ, Huang J, James DF (2001) An inter-laboratory comparison of measurements from filament stretching rheometers using common test fluids. J Rheol 45:83–114

Appell J, Porte G, Khatory A, Kern F, Candau SJ (1992) Static and dynamic properties of a network of wormlike surfactant micelles (etylpyridinium chlorate in sodium chlorate brine). J Phys II 2:1045–1052

Bazilevsky AV, Entov VM, Rozhkov AN, Yarin AL (1990) Polymer jets, beans-on-string breakup and related phenomena. In: third European Rheology conference

Berret J-F (1997) Transient rheology of wormlike micelles. Langmuir 13:2227–2234

Berret J-F, Appell J, Porte G (1993) Linear rheology of entangled wormlike micelles. Langmuir 9:2851–2854

Bhardwaj A, Miller E, Rothstein JP (2007) Filament stretching and capillary breakup extensional rheometry measurements of visco-elastic wormlike micelle solutions. J Rheol (in press)

Bird RB, Armstrong RC, Hassager O (1987) Dynamics of polymeric liquids: vol. 1 fluid mechanics. John Wiley & Sons, New York

Britton MM, Callaghan PT (1999) Shear banding instability in wormlike micellar solutions. Eur Phys J B 7:237–249

Cappelaere E, Berret J-F, Decruppe JP, Cressely R, Lindner P (1997) Rheology, birefringence, and small angle neutron scattering in a charged micellar system: evidence of shear-induced phase transition. Phys Rev E 56:1869–1878

Cates ME (1987) Reptation of living polymers: dynamics of entangled polymers in the presence of reversible chain-scission reactions. Macromolecules 20:2289–2296

Cates ME (1990) Nonlinear viscoelasticity of wormlike micelles (and other reversibly breakable polymers). J Phys Chem 94:371–375

Cates ME, Turner MS (1990) Flow-induced gelation of rodlike micelles. Europhys Lett 11:681–686

Chen S, Rothstein JP (2004) Flow of a wormlike micelle solution past a falling sphere. J Non-Newton Fluid Mech 116:205–234

Chen C, Warr GG (1997) Light scattering from wormlike micelles in an elongational flow. Langmuir 13:1374–1376

Cooper-White JJ, Crooks RC, Boger DV (2002) A drop impact study of worm-like viscoelastic surfactant solutions. Colloids Surf A Physicochem Eng Asp 210:105–123

Decruppe JP, Ponton A (2003) Flow birefringence, stress optical rule and rheology of four micellar solutions with the same low shear viscosity. Eur Phys J E 10:201–207

Doi M, Edwards SF (1986) The theory of polymer dynamics. Oxford University Press, Oxford

Doyle PS, Shaqfeh ESG, McKinley GH, Spiegelberg SH (1998) Relaxation of dilute polymer solutions following extensional flow. J Non-Newton Fluid Mech 76:79–110

Drappier J, Bonn D, Meunier J, Lerouge S, Decruppe JP, Bertrand F (2006) Correlation between birefringent bands and shear bands in surfactant solutions. J Stat Mech Theory Exp P04003

Entov VM, Hinch EJ (1997) Effect of a spectrum of relaxation times on the capillary thinning of a filament of elastic liquid. J Non-Newton Fluid Mech 72:31–53

Fischer E, Callaghan PT (2001) Shear banding and the isotropic-to-nematic transition in wormlike micelles. Phys Rev E 64:011501

Fischer P, Rehage H (1997) Rheological master curves of viscoelastic surfactant solutions by varying the solvent viscosity and temperature. Langmuir 13:7012–7020

Fischer P, Fuller GG, Lin Z (1997) Branched viscoelastic surfactant solutions and their responses to elongational flow. Rheol Acta 36:632–638

Grand C, Arrault J, Cates ME (1997) Slow transients and metastability in wormlike micelle rheology. J Phys II 7:1071–1086

Granek R, Cates ME (1992) Stress relaxation in living polymers: results from a Poisson renewal model. J Chem Phys 96:4758–4767

Handzy NZ, Belmonte A (2004) Oscillatory rise of bubbles in wormlike micellar fluids with different microstructures. Phys Rev Lett 92:124501

Hu Y, Wang SQ, Jamieson AM (1993) Rheological and flow birefringence studies of a shear-thickening complex fluid—A surfactant model system. J Rheol 37:531–546

Huang CM, JJ Magda RG Larson D Pine CH Liu (1996) Shear flow rheology of micellar solutions containing 'Living' polymer

chains. Proceedings of the XIIth international congress on rheology 217–218

In M, Warr GG, Zana R (1999) Dynamics of branched threadlike micelles. Phys Rev Lett 83:2278–2281

Israelachvili JN (1985) Intermolecular and surface forces: with applications to colloidal and biological systems. Academic, London

James DF, McLean BD, Saringer JH (1987) Presheared extensional flow of dilute polymer solutions. J Rheol 31:453–481

Jayaraman A, Belmonte A (2003) Oscillations of a solid sphere falling through a wormlike micelle solution. Phys Rev E 67:065301

Kadoma IA, van Egmond JW (1998) Flow-induced nematic string phase in semidilute wormlike micelle solutions. Phys Rev Lett 80:5679–5682

Kato M, Takahashi T, Shirakashi M (2002) Steady planar elongational viscosity of CTAB/NaSal aqueous solutions measured in a 4-roll mill flow cell. J Soc Rheol Jpn 30:283–287

Kato M, Takahashi T, Shirakashi M (2004) "Flow-induced structure change and flow instability of CTAB/NaSal aqueous solution in 4-roll mill flow cell." In: Int Congr on Rheol, Seoul, Korea

Kefi S, Lee J, Pope T, Sullivan P, Nelson E, Hernandez A, Olsen T, Parlar M, Powers B, Roy A, Wilson A, Twynam A (2004) Expanding applications for viscoelastic surfactants. Oilfield Rev 10–16

Kern F, Lequeux F, Zana R, Candau SJ (1994) Dynamics properties of salt-free viscoelastic micellar solutions. Langmuir 10:1714–1723

Khatory A, Lequeux F, Kern F, Candau SJ (1993) Linear and nonlinear viscoelasticity of semidilute solutions of wormlike micelles at high salt concentration. Langmuir 9:1456–1464

Larson RG (1999) The structure and rheology of complex fluids. Oxford University Press, New York

Larson RG (2000) The role of molecular folds and "pre-conditioning" in the unraveling of polymer molecules during extensional flow. J Non-Newton Fluid Mech 94:37–45

Larson RG (2005) The rheology of dilute solutions of flexible polymers: progress and problems. J Rheol 49:1–70

Lee JY, Fuller GG, Hudson NE, Yuan X-F (2005) Investigation of shear-banding structure in wormlike micellar solution by point-wise flow-induced birefringence measurements. J Rheol 49:537–550

Lequeux F, Candau SJ (1997) "Structural properties of wormlike micelles." In: McLeish T (ed) Theoretical challenges in the dynamics of complex fluids. Kluwer Academic Publishers, Netherlands

Lerouge S, Decruppe JP (2000) Correlations between rheological and optical properties of a micellar solution under shear banding flow. Langmuir 16:6464–6474

Lu B, Li X, Scriven LE, Davis HT, Talmon Y, Zakin JL (1998) Effect of chemical structure on viscoelasticity and extensional viscosity of drag-reducing cationic surfactant solutions. Langmuir 14:8–16

Mair RW, Calaghan PT (1996) Observation of shear banding in worm-like micelles by NMR velocity imaging. Europhys Lett 36:719–724

McKinley GH, Sridhar T (2002) Filament stretching rheometry. Annu Rev Fluid Mech 34:375–415

McKinley GH, Tripathi A (2000) How to extract the Newtonian viscosity from capillary breakup measurements in a filament rheometer. J Rheol 44:653–670

Mendez-Sanchez A, Perez-Gonzalez J, de Vargas L, Castrejon-Pita JR, Castrejon-Pita AA, Huelsz G (2003) Particle image velocimetry of the unstable capillary flow of a micellar solutions. J Rheol 47:1455–1466

Miller E, Rothstein JP (2007) Transient evolution of shear banding in wormlike micelle solutions. J Non-Newton Fluid Mech (in press)

Miller E, Lee SJ, Rothstein JP (2006) The effect of temperature gradients on the sharkskin surface instability in polymer extrusion through a slit die. Rheol Acta 45:943–950

Mollinger AM, Cornelissen EC, van den Brule BHAA (1999) An unexpected phenomenon observed in particle settling: oscillating falling spheres. J Non-Newton Fluid Mech 86:389–393

Muller AJ, Torres MF, Saez AE (2004) Effect of the flow field on the rheological behavior of aqueous cetyltrimethylammonium p-toluenesulfonate solutions. Langmuir 20:3838–3841

Papageorgiou DT (1995) On the breakup of viscous liquid threads. Phys Fluids 7:1529–1544

Prud'homme RK, Warr GG (1994) Elongational flow of solutions of rodlike micelles. Langmuir 10:3419–3426

Rehage H, Hoffmann H (1991) Viscoelastic surfactant solutions: model systems for rheological research. Mol Phys 74:933–973

Rodd LE, Scott TP, Cooper-White JJ, McKinley GH (2005) Capillary break-up rheometry of low-viscosity elastic fluids. Appl Rheol 15:12–27

Rothstein JP (2003) Transient extensional rheology of wormlike micelle solutions. J Rheol 47: 1227–1247

Rothstein JP, McKinley GH (2001) The axisymmetric contraction-expansion: The role of extensional rheology on vortex growth dynamics and the enhanced pressure drop. J Non-Newton Fluid Mech 98:33–63

Rothstein JP, McKinley GH (2002a) A comparison of the stress and birefringence growth of dilute, semi-dilute and concentrated polymer solutions in uniaxial extensional flows. J Non-Newton Fluid Mech 108:275–290

Rothstein JP, McKinley GH (2002b) Inhomogeneous transient uniaxial extensional rheometry. J Rheol 46:1419–1443

Shikata T, Kotaka T (1991) Entanglement network of thread-like micelles of a cationic detergent. J Non-Cryst Solids 131–133:831–835

Smith DE, Chu S (1998) Response of flexible polymers to a sudden elongational flow. Science 281:1335–1340

Smolka LB, Belmonte A (2003) Drop pinch-off and filament dynamics of wormlike micellar fluids. J Non-Newton Fluid Mech 115:1–25

Sridhar T, Tirtaatmadja V, Nguyen DA, Gupta RK (1991) Measurement of extensional viscosity of polymer solutions. J Non-Newton Fluid Mech 40:271–280

Stelter M, Brenn G, Yarin AL, Singh RP, Durst F (2000) Validation and application of a novel elongational device for polymer solutions. J Rheol 44:595–616

Szabo P (1997) Transient filament stretching rheometry I: force balance analysis. Rheol Acta 36:277–284

Tirtaatmadja V, Sridhar T (1993) A filament stretching device for measurement of extensional viscosity. J Rheol 37:1133–1160

Tripathi A, McKinley GH, Tam KC, Jenkins RD (2006) Rheology and dynamics of associative polymers in shear and extension: theory and experiments. Macromol 39:1981–1999

Vissmann K, Bewersdorff H-W (1990) The influence of pre-shearing on the elongational behavior of dilute polymer and surfactant solutions. J Non-Newton Fluid Mech 34:289–317

Walker LM, Moldenaers P, Berret J-F (1996) Macroscopic response of wormlike micelles to elongational flow. Langmuir 12:6309–6314

Wheeler EK, Fischer P, Fuller GG (1998) Time-Periodic flow induced structures and instabilities in a Viscoelastic surfactant solution. J Non-Newton Fluid Mech 75:193–208

Yesilata B, Clasen C, McKinley GH (2006) Nonlinear shear and extensional flow dynamics of wormlike surfactant solutions. J Non-Newton Fluid Mech 133:73–90